SEVA: An externally driven framework for reproducing COVID-19 mortality waves without transmission feedback

Short title: SEVA model of COVID-19 mortality waves

Kim Varming

Aalborg, Denmark

E-mail: varming.kim@gmail.com

Abstract

Background

COVID-19 epidemic waves display pronounced temporal structure in mortality, with substantial variation in wave shape, duration, and asymmetry across regions. These dynamics are commonly interpreted within transmission-based compartmental models, in which epidemic growth is driven by interactions between infectious and susceptible individuals. However, several empirical features of observed mortality curves, including prolonged declines, asymmetric wave shapes, and coherent temporal patterns across regions with differing interventions, are difficult to reconcile within a purely transmission-driven framework.

Methods

We introduce and evaluate an externally driven epidemic model, termed the Seasonally and Environmentally driven Virus Activity (SEVA) framework. In SEVA, epidemic dynamics are governed by a time-varying, population-averaged probability

of infection that is independent of the number of infected individuals and does not generate transmission feedback. Because infection events are not directly observable, the model is extended to simulate mortality and calibrated to daily COVID-19 death data.

Results

Across multiple European countries and U.S. states during the first epidemic wave in spring 2020, the SEVA framework reproduces the dominant temporal features of observed mortality curves, including peak timing, wave width, and overall curve morphology. Modest variation in a single parameter, the maximum activity level, accounts for both sharply peaked mortality waves and broader, more prolonged waves. This agreement is achieved without region-specific transmission coefficients, contact structures, or intervention-dependent parameterization.

Conclusions

These findings demonstrate that externally driven, population-level exposure dynamics provide a parsimonious and empirically adequate description of early COVID-19 mortality wave morphology. By decoupling epidemic dynamics from transmission feedback, the SEVA framework offers a complementary perspective on epidemic wave formation and highlights the potential importance of seasonal and environmental modulation of viral activity. Identifying the mechanisms underlying such modulation represents an important direction for future research.

Introduction

Epidemic waves of COVID-19 have exhibited pronounced temporal structure in mortality, with substantial variation in wave shape, duration, and asymmetry across regions. Since the start of the pandemic, these dynamics have predominantly been interpreted within transmission-based compartmental frameworks, such as SIR and related models, in which epidemic growth is driven by interactions between infectious and susceptible individuals and modulated by behavioral change, public health interventions, and depletion of susceptibles [1-3].

While such models have been successful in describing short-term transmission processes, several empirical features of COVID-19 mortality waves remain difficult to reconcile within a purely transmission-driven framework. In particular, mortality curves often display rapid resolution even in the absence of clear evidence for sustained intervention effects [4-5], and epidemic waves across regions frequently show coherent temporal structure despite large differences in policy measures, population behavior, and assumed contact patterns [6-7].

These observations motivate consideration of alternative modeling perspectives that focus on population-level exposure dynamics rather than explicit person-to-person transmission. Seasonal and environmental modulation of respiratory virus activity has long been recognized for influenza and other respiratory pathogens [8-10] yet such effects are typically incorporated implicitly or treated as secondary modifiers of transmission parameters. The extent to which externally driven variation in population-level infection probability alone can account for observed epidemic wave structure remains insufficiently explored.

In this study, we introduce and evaluate a simple externally driven epidemic framework, termed the Seasonally and Environmentally driven Virus Activity (SEVA) model. In SEVA, epidemic waves are governed by a time-varying, population-

averaged probability of infection that is independent of the number of infected individuals. Individuals enter an infected compartment in response to this externally specified activity term, but do not generate secondary infections within the model. As a consequence, epidemic dynamics arise without transmission-based feedback, and depletion of susceptibles does not play the same mechanistic role as in classical SIR-type models.

Importantly, the SEVA framework does not specify the biological or environmental mechanisms underlying changes in viral activity. Instead, it treats variation in infection probability as an empirical driver inferred from population-level outcomes. This study therefore does not seek to identify the causal origin of activity modulation, but rather to assess whether such modulation, irrespective of mechanism, is sufficient to account for observed epidemic wave morphology.

This deliberate abstraction allows the model to be evaluated directly against observed data without presupposing specific causal pathways, such as behavioral change, policy interventions, or individual contact structure [11].

Because population-level infection data are not directly observable, we calibrate the model to daily COVID-19 mortality, which represents the most consistently recorded endpoint across regions and time [12]. By extending the SEVA framework to include mortality as an outcome of infection, we assess whether externally driven exposure dynamics alone can reproduce the dominant temporal features of observed mortality curves.

We apply this approach to multiple European countries and U.S. states during the first epidemic wave of COVID-19. Model performance is evaluated using both visual comparison and standard quantitative measures of curve similarity. Particular

attention is given to systematic regional differences in epidemic wave shape, including the contrast between sharply peaked and more prolonged mortality curves. The primary objective of this study is not to identify the biological origin of seasonal or environmental modulation of viral activity, but to test whether such modulation, treated as an external, population-level driver, provides a parsimonious and empirically adequate description of observed epidemic dynamics. By explicitly contrasting the SEVA framework with classical transmission-based models at the level of infection dynamics, we aim to clarify which features of COVID-19 mortality waves can be reproduced without transmission feedback and which aspects, specifically the mechanisms underlying activity modulation, remain unresolved.

Methods

Simulation environment

All simulations were implemented using *Stella Architect* (ISEE Systems, Lebanon, NH, USA), a system dynamics modelling environment based on explicit stock–flow formulations and numerical time integration.

Model simulations were run using fixed time steps and standard Euler integration. The time step, and numerical solver settings were kept identical across all runs and regions.

For transparency and reproducibility, the full set of core simulation settings used in *Stella Architect*, including run specifications, time step, integration method, and the functional form of the external activity driver, are provided in Supplementary (S1 Fig)

Model overview

Epidemic waves in the SEVA framework are driven by an externally specified, time-varying activity term that represents population-averaged seasonal and environmental modulation of viral exposure consistent with established evidence for climate- and environment-related forcing of respiratory virus activity [9-10]. This activity term governs the rate at which individuals enter an infected compartment. Importantly, the infected compartment does **not** represent infectiousness in the classical epidemiological sense and does not generate secondary cases. Consequently, the size of the infected compartment does not feed back into the rate of new infections (Fig 1), in contrast to transmission-based compartmental models.[1,3].

Mathematical formulation.

The daily inflow into the infected compartment is defined as

Infected per day(t) = Susceptible(t) * p_infection per day(t)

where (p_infection per day(t)) follows a sigmoidal increase over 40 days from zero to a maximum value (p_max). Sigmoidal forcing functions are commonly used to represent gradual onset of external drivers in dynamical systems when mechanistic detail is unavailable [13].

Fig 1 Basic structure of the SEVA infection model.

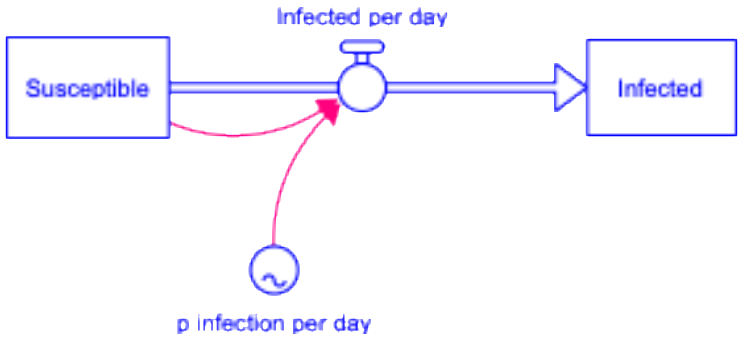

The model consists of two stocks (susceptible and infected), one flow, and one connector. Susceptible individuals enter the infected compartment at a rate determined by an externally specified, time-varying probability of infection per day (p_infection per day) which increases sigmoidally over time toward a maximum value (p_max). The infected compartment does not represent infectiousness and does not generate secondary infections.

Comparison of the SEVA model with SIR-type models

Conceptual comparison of infection dynamics

To facilitate interpretation of the empirical mortality curves presented in the Results section—particularly the pronounced differences between northern and southern U.S. states—we contrast the infection dynamics implied by classical transmission-based SIR models with those of the externally driven SEVA framework.

In classical SIR models, epidemic trajectories arise from feedback between infectious and susceptible individuals. The rate of new infections depends on the current number of infectious individuals, producing nonlinear epidemic waves that are constrained by depletion of susceptibles and accumulation of immunity (Fig 2).

In contrast, SEVA prescribes a time-varying, population-averaged probability of infection that is independent of the number of infected individuals. Individuals enter

the infected compartment in response to an externally modulated activity term, and the infected compartment does not participate in any positive feedback mechanism. Epidemic dynamics are therefore governed by the magnitude and temporal evolution of the external activity rather than by transmission feedback.

This structural distinction has direct implications for epidemic curve morphology. At low maximum activity levels (p_max), only a limited fraction of the population becomes infected within a given time window, producing broad, slowly declining epidemic waves that do not reach saturation. At higher activity levels, a large fraction of the population may become infected over a short period, yielding sharply peaked curves followed by rapid decline once a large fraction of the population has been infected. This conceptual difference anticipates the regional mortality patterns observed in the Results section.

Fig 2 Structure of a classical SIR model.

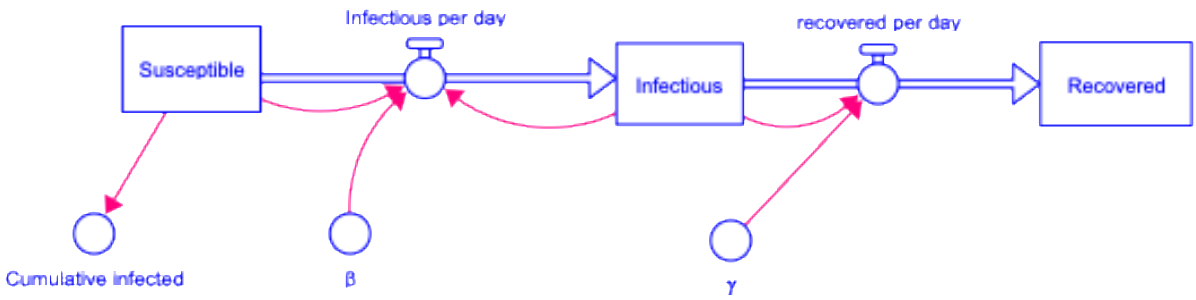

The model consists of susceptible, infectious, and recovered compartments connected by transmission- and recovery-driven flows. New infections depend on interactions between susceptible and infectious individuals, generating positive feedback and nonlinear epidemic dynamics.

Simulation of infection dynamics

In classical SIR models, infection dynamics are governed by the parameters β and γ where β represents the probability of infection per contact per day and γ the daily probability of recovery or death. The ratio β / γ defines the basic reproduction number R_0, which for COVID-19 has typically been estimated to lie between 2 and 6 [14].

In SEVA, infection dynamics depend instead on the maximum population-averaged probability of infection per day (p_max) and on the duration of the external activity increase.To illustrate the combined effects of the maximum activity level (p_max) and the duration of the sigmoidal increase in activity, we performed a series of exploratory simulations in which p_max and rise time were varied independently. Figure 4 shows simulations for two representative activity regimes (p_max = 0.002 and p_max = 0.05) and three rise times (20, 40, and 60 days). These simulations demonstrate that the timing and width of the peak in daily infections are jointly determined by p_max and the duration of the activity increase, and that peak characteristics alone are insufficient to uniquely identify either parameter.

(Fig 3) and (Fig 4) illustrate how variation in β (SIR) and (p_max) (SEVA), respectively, produces qualitatively different epidemic trajectories, demonstrating that both broad and sharply peaked epidemic waves can arise in SEVA without invoking changes in transmission efficiency or contact structure.
These simulations provide an interpretative framework for the regional mortality curve shapes analyzed in the Results section.

209 **Fig 3 Simulation with a classical SIR model of COVID-19 infections over 200**

210 **days.**

211 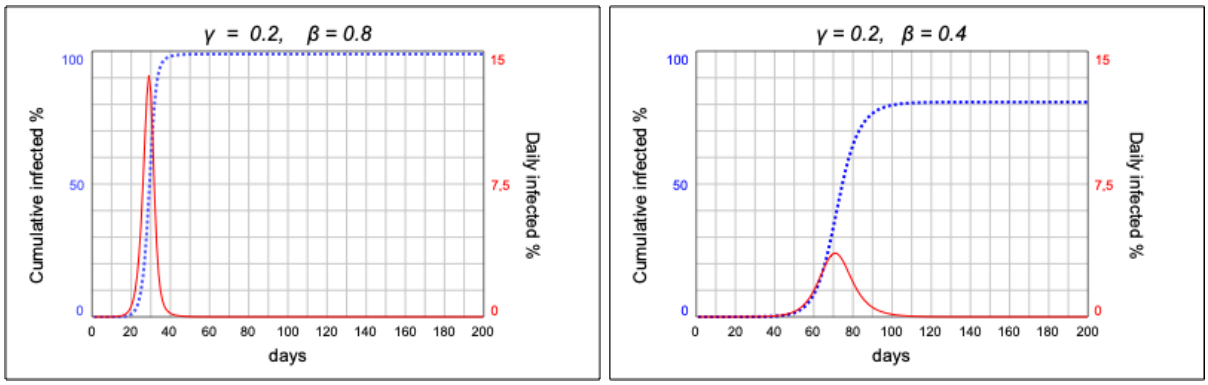

212 The recovery parameter *γ* is fixed at 0.2. Reducing *β* from 0.8 to 0.4 flattens and

213 delays the epidemic peak and reduces the total fraction infected.

214

215 **Fig 4 Simulation with the SEVA model of COVID-19 infections over 200 days.**

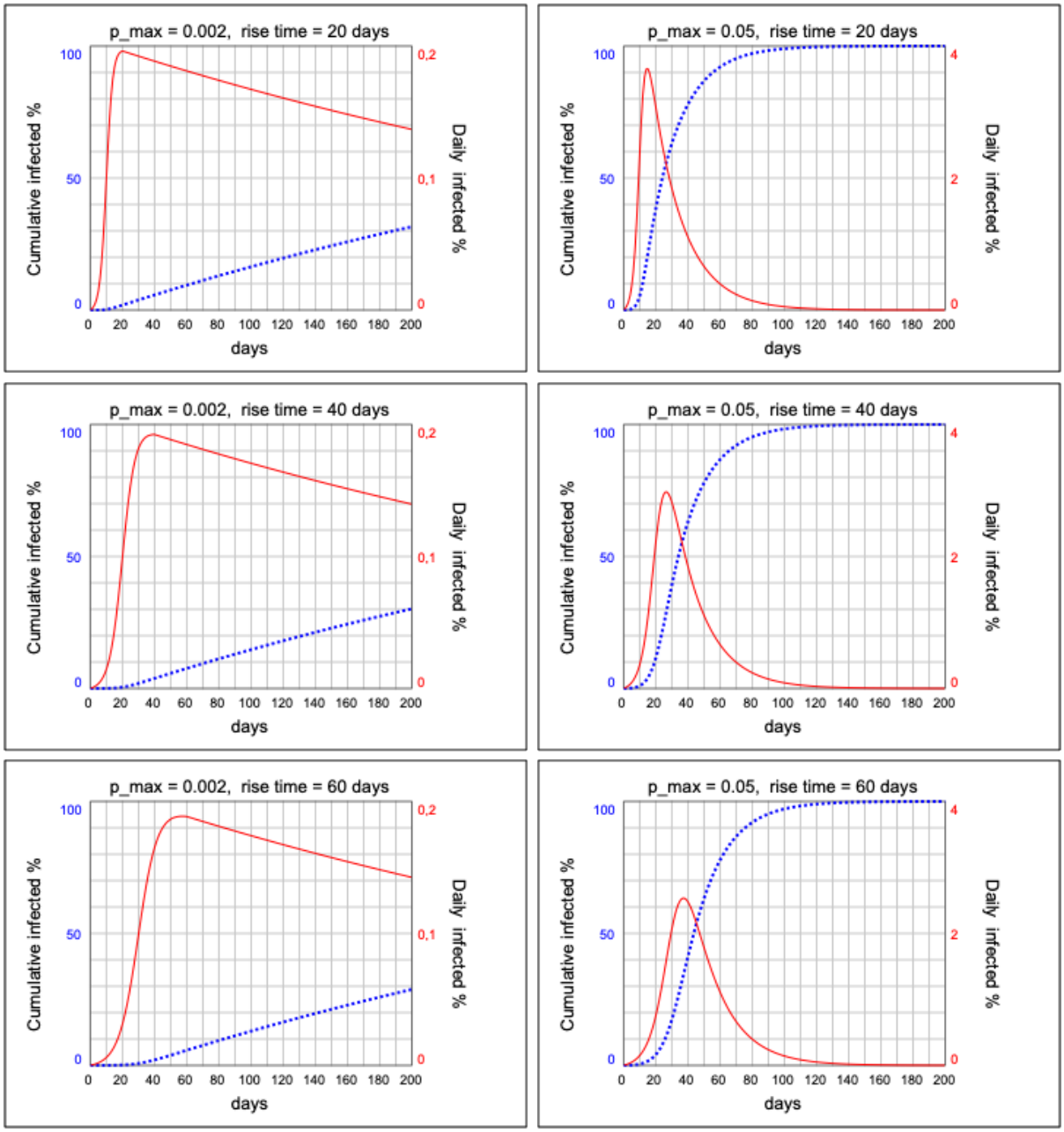

The duration of the sigmoidal activity increase varies between 20, 40, and 60 days. Reducing (p_max) from 0.05 to 0.002 produces flatter infection curves, lower peak intensity, and a reduced fraction infected within the simulation window, with the daily infection curve becoming increasingly right-skewed.

Extension to mortality modeling

Because population-level infection data are not directly observable, the SEVA framework was extended to simulate COVID-19 mortality. Individuals enter the infected compartment according to the external activity term and exit through two mutually exclusive flows: death or survival. Daily deaths are modeled as a fixed per-day fraction of the infected population, while survivors accumulate in a separate stock, ensuring conservation of population mass.

Mathematical formulation.

Deaths per day(t) = Infected(t) * p_dead per day(t)

with survival defined as the complementary outcome.

Fig 5 Structure of the SEVA-based mortality model.

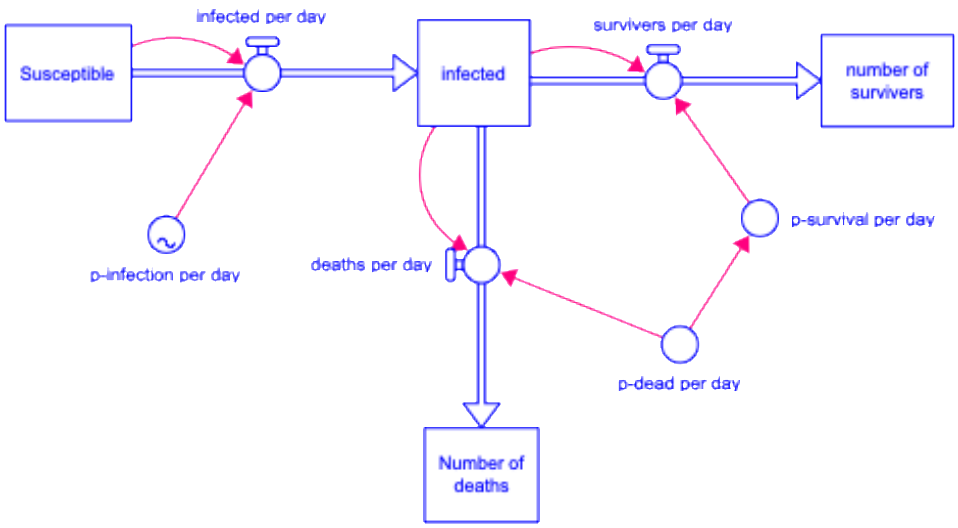

The model consists of stocks representing susceptible individuals, infected individuals, cumulative deaths, and survivors, connected by flows governed by externally specified probabilities. Arrows indicate causal connections between model

components.

Immunity, observability, and timing

Individual-level immunity and heterogeneity in susceptibility are not explicitly parameterized. Because the infected compartment does not participate in positive feedback, depletion of susceptibles does not play the same dynamical role as in transmission-based models. At the population level, immune protection and heterogeneity are implicitly reflected in the observed mortality curves used for calibration.

Infection events are not directly observable in population data, and the calendar start time of epidemic waves is generally unknown. Model–data comparisons therefore rely on temporal alignment. Under these conditions, explicit modeling of delays from infection to death is not separately identifiable from a time shift and would not alter the inferred curve shapes.

Data sources

Observed COVID-19 mortality data for European countries were obtained from the European Centre for Disease Prevention and Control (ECDC) COVID-19 surveillance database [15].

Mortality data for U.S. states were obtained from the COVID Tracking Project, which

provides harmonized, state-level daily death counts compiled from official state and territorial health authorities [16].

Mortality counts were converted to deaths per 100,000 population and smoothed using a 7-day running average prior to model calibration.

Calibration and evaluation

In initial exploratory simulations, rise times in the range of 20–60 days were evaluated. A rise time of approximately 40 days was found to provide a robust and generally applicable representation of the onset phase across regions. This value was therefore adopted as a common default setting in all subsequent simulations.
Model calibration was performed in two sequential steps to disentangle mortality scaling from epidemic curve shape.
First, the per-day mortality parameter (p_dead per day) was adjusted such that the cumulative number of simulated deaths over the analysis window matched the observed cumulative COVID-19 mortality for each country or U.S. state. This step ensures that differences in overall mortality magnitude are accounted for independently of the temporal dynamics of the epidemic wave.
Second, with cumulative mortality fixed, the maximum activity parameter (p_max) was adjusted to reproduce the temporal shape of the observed daily mortality curve, including peak height, wave width, and rate of decline. No additional parameters were modified at this stage.
This calibration strategy allows the temporal dynamics of mortality to be evaluated independently of absolute mortality levels and ensures that variation in epidemic

wave shape is attributed to differences in the external activity profile rather than to differences in mortality scaling.

Results

Reproduction of COVID-19 mortality curves in Europe

Figure 6 shows the observed and modelled daily COVID-19 mortality rates (7-day running mean, per 100,000 population) for selected European countries during the first epidemic wave.

For comparability, all European time series were aligned to a common calendar start date (8 March 2020), rather than to the first recorded COVID-19 death in each country. This alignment facilitates direct comparison of peak timing and overall curve morphology across regions. As a consequence, the early portions of some curves include periods with zero or near-zero mortality.

Across all included European countries, the SEVA model reproduces the overall epidemic trajectory well, capturing both the rapid rise and the subsequent decline in daily mortality. Peak timing and peak daily mortality magnitude are well reproduced. with only modest deviations around the apex in some countries. The declining phase is well described, exhibiting a smooth and monotonic decrease

exhibiting a smooth and monotonic decrease that closely follows the empirical data. Quantitative goodness-of-fit metrics calculated over a fixed 100-day analysis window (starting from the first day with non-zero mortality in each country) demonstrate consistently high agreement between model output and observed data (Table 1). Coefficients of determination (R^2) are high across all European countries, and error metrics (RMSE and MAE) remain low.

These results indicate that the SEVA framework captures the dominant temporal structure of the epidemic through country-specific adjustment of the maximum activity parameter (p_max), while cumulative mortality is matched separately through a single mortality scaling parameter and does not influence curve shape.

Corresponding SEVA model fits for an additional 13 European countries are provided in (S2 Fig) indicating that the ability of the SEVA framework to reproduce first-wave mortality dynamics extends beyond the countries shown in (Fig 6).

Fig 6. Reproduction of COVID-19 mortality curves in selected European countries using the SEVA model.

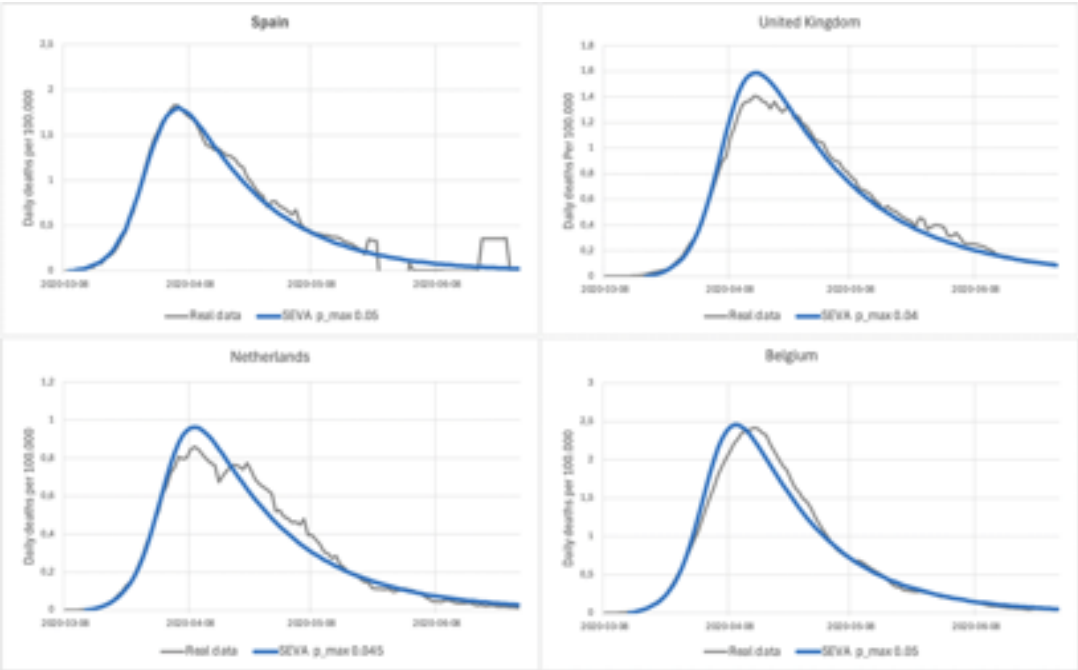

Observed daily COVID-19 mortality (7-day running average, deaths per 100,000 population) is shown together with corresponding SEVA model outputs for selected European countries during the first epidemic wave in spring 2020.
All curves are temporally aligned to a common calendar date (8 March 2020) to allow direct comparison of curve shape and timing.

Despite differences in population size, reporting practices, and public health responses, the SEVA model reproduces the characteristic rise, peak, and decline of mortality across countries using the same model structure. Differences in curve morphology are accounted for by variation in the maximum activity parameter (p_max).

Regional mortality patterns in the United States

Fig 7. presents corresponding results for selected U.S. states. As for Europe, the curves represent daily mortality rates smoothed by a 7-day running mean, but are here aligned to a common calendar start date of 15 March 2020, reflecting the later onset of the epidemic in the United States.

The SEVA model reproduces the main temporal features of the first epidemic wave in the selected U.S. states. In all cases, the model captures the overall rise, peak, and subsequent decline of daily COVID-19 mortality.

Fit metrics for all U.S. states are summarised in Table 1 and were computed using the same 100-day analysis window and methodological criteria as for the European analyses. While coefficients of determination (R^2) are generally slightly lower in southern U.S. states — reflecting increased reporting, variability and temporal irregularity,

particularly during the post-peak phase — overall model performance remains robust across regions.

Fig 7. Regional contrast in COVID-19 mortality dynamics between northern and southern U.S. states reproduced by the SEVA model.

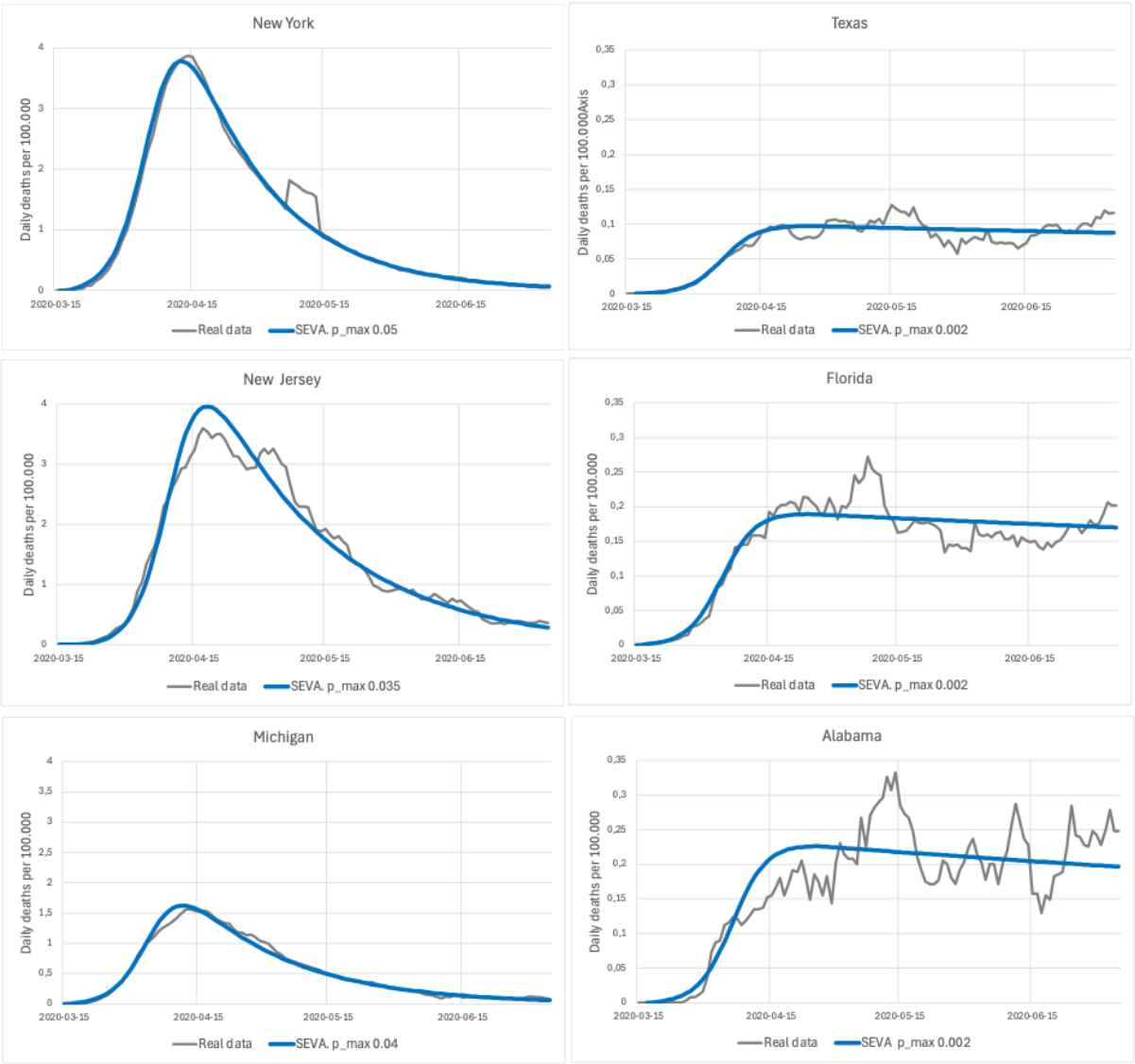

Observed daily COVID-19 mortality (7-day running average, deaths per 100,000 population) and corresponding SEVA model outputs are shown for representative northern U.S. states (Panel A) and southern U.S. states (Panel B) during the first epidemic wave in 2020.

All curves are temporally aligned to a common calendar date (15 March 2020). Northern states exhibit sharply peaked mortality curves with rapid rise and decline, whereas southern states show broader and more prolonged mortality profiles with lower peak intensity. These regional differences emerge in the SEVA model without

changes to the underlying model structure and are driven by variation in the external virus activity profile (p_max), rather than by differences in transmission parameters.

Summary of fit performance

Across both European countries and U.S. states, the SEVA model consistently reproduces the first-wave dynamics of COVID-19 daily mortality using a unified modelling framework.

All temporal agreement between model output and empirical data reflects variation in the maximum activity parameter (p_max), as cumulative mortality is matched separately through adjustment of the per-day mortality parameter (p_dead per day) prior to evaluation of curve shape.

Consequently, goodness-of-fit metrics quantify agreement in epidemic timing and morphology rather than differences in total mortality burden.

The results demonstrate that a common, externally synchronised temporal framework can yield strong agreement between model and data across diverse regions without region-specific tuning of transmission parameters or epidemic onset dates.

Table 1. Quantitative agreement between observed and simulated COVID-19 mortality curves.

Region	p_max	RMSE	MAE	R2	Pearson_r
Belgium	0,050	0,14	0,09	0,97	0,98
Netherlands	0,045	0,07	0,05	0,95	0,98
Spain	0,050	0,15	0,10	0,94	0,97
UK	0,035	0,05	0,04	0,99	0,99
Michigan	0,040	0,06	0,04	0,98	0,99
New Jersey	0,035	0,24	0,18	0,96	0,98
New York State	0,050	0,23	0,14	0,96	0,98
Alabama	0,002	0,04	0,04	0,59	0,77
Florida	0,002	0,02	0,02	0,88	0,94
Texas	0,002	0,01	0,01	0,86	0,93

Goodness-of-fit between observed daily COVID-19 mortality (7-day running average) and SEVA model outputs was assessed using RMSE, MAE, and coefficient of determination (R^2). Fit metrics were calculated for each country and U.S. state over a fixed 100-day analysis window using temporally aligned mortality curves.

The metrics indicate close agreement between model and data across diverse geographic regions, with remaining differences primarily reflecting reporting noise and variation in epidemic wave shape rather than systematic model mismatch.

Discussion

In this study, we introduced and evaluated the SEVA framework, an externally driven epidemic model in which population-level infection dynamics are governed by a time-varying activity term rather than by transmission feedback between infected and susceptible individuals. Using COVID-19 mortality data from multiple European countries and selected U.S. states during the first epidemic wave in spring 2020, we show that this parsimonious framework reproduces the dominant temporal features of observed mortality curves across markedly different regions.

Interpretation of the main findings

A central finding is that a single model structure, combined with modest variation in the maximum activity parameter (p_max), is sufficient to reproduce both sharply peaked mortality waves—typical of several northern U.S. states and parts of Europe—and broader, more slowly declining waves characteristic of southern U.S. states. Importantly, these differences emerge without explicitly invoking region-specific transmission coefficients, contact structures, or explicit intervention effects, which are commonly emphasized in transmission-based models [1–3].

Within the SEVA framework, epidemic wave termination is not driven by collapse of transmission through feedback or behavioral change, but by the interaction between the externally prescribed activity profile and the progressive exposure of the susceptible population during periods of elevated activity. In regions with low p_max, only a limited fraction of the population becomes infected within the analyzed time window, resulting in prolonged and asymmetric epidemic waves. In contrast, higher p_max values lead to rapid exposure of a large population fraction, producing sharply peaked mortality curves followed by decline.

This interpretation provides a coherent explanation for the pronounced north–south contrast observed in U.S. mortality curves during spring 2020, which emerged despite substantial heterogeneity in public health interventions and population behavior across states.

Relation to classical transmission-based models

Classical SIR-type models attribute epidemic dynamics to nonlinear feedback between infectious and susceptible individuals, with epidemic peaks emerging from transmission amplification and declines driven by depletion of susceptibles and accumulation of immunity [1,2]. While such models are mechanistically appropriate for describing individual-level transmission processes, they implicitly assume that population-level epidemic patterns are primarily governed by interpersonal transmission intensity.

The SEVA framework does not deny that individual infections occur, nor that such infections may involve person-to-person contact. In SEVA, the timing, width, and resolution of epidemic waves emerge from externally modulated population-wide exposure, rather than from transmission-based feedback between infected and susceptible individuals. Thus, transmission events may occur at the individual level, but they do not constitute the dominant driver of epidemic wave dynamics at the population scale within this framework.

Implications for epidemic seasonality and environmental modulation

One implication of this work is that seasonal or environmental modulation of viral activity may play a more central role in shaping epidemic waves than is typically acknowledged in transmission-centered frameworks. Seasonal patterns have long been recognized for respiratory viruses, including influenza and endemic coronaviruses, but are often incorporated only implicitly through time-varying transmission parameters [8–10].

The SEVA model deliberately does not specify the biological or environmental mechanisms underlying the activity term; instead, it infers their aggregate population-level effect from observed mortality data. At present, empirical understanding of what drives seasonal increases in population-level infection probability remains limited. Potential contributors may include environmental stability of viral particles, host susceptibility, immune modulation, or indirect behavioral factors, but the present analysis does not depend on any specific mechanism.

Identifying the biological and environmental determinants of population-level viral activity therefore emerges as a critical research priority, particularly in light of the strong empirical regularities captured by the SEVA framework.

Methodological strengths and limitations

A major strength of this study is its reliance on mortality data, which represent the most consistently recorded and comparable epidemic endpoint across regions during early 2020 [12]. By focusing on curve shape and relative timing rather than absolute epidemic onset, the analysis avoids assumptions about poorly identifiable delays from infection to death, which are known to vary substantially across settings.

Several limitations should be noted. First, the SEVA framework is intentionally phenomenological at the population level and does not resolve individual-level transmission processes or heterogeneity. Second, the external activity term is inferred indirectly and does not identify underlying causal mechanisms. Third, the analysis is restricted to the first

epidemic wave and does not address later waves influenced by vaccination, viral evolution, or changing immunity landscapes.

These limitations are inherent to the study's objective: to test whether externally driven exposure dynamics can account for observed epidemic wave morphology, rather than to provide a complete mechanistic description of viral transmission.

Conclusions

This study demonstrates that a simple, externally driven epidemic framework can reproduce a wide range of COVID-19 mortality wave shapes observed during the first epidemic wave across Europe and the United States. By decoupling epidemic dynamics from transmission feedback, the SEVA model offers a complementary perspective on epidemic wave formation and resolution.

References

1. Kermack WO, McKendrick AG. A contribution to the mathematical theory of epidemics. *Proc R Soc Lond A*. 1927;115:700–721. doi:10.1098/rspa.1927.0118
2. Anderson RM, May RM. *Infectious diseases of humans: dynamics and control*. Oxford: Oxford University Press; 1991.
3. Keeling MJ, Rohani P. *Modeling infectious diseases in humans and animals*. Princeton (NJ): Princeton University Press; 2008.

4. Brauner JM, Mindermann S, Sharma M, Johnston D, Salvatier J, Gavenčiak T, et al. Inferring the effectiveness of government interventions against COVID-19. *Science*. 2021;371(6531):eabd9338. doi:10.1126/science.abd9338
5. Flaxman S, Mishra S, Gandy A, Unwin HJT, Mellan TA, Coupland H, et al. Estimating the effects of non-pharmaceutical interventions on COVID-19 in Europe. *Nature*. 2020;584(7820):257–261. doi:10.1038/s41586-020-2405-7
6. Ioannidis JPA, Cripps S, Tanner MA. Forecasting for COVID-19 has failed. *Int J Forecast*. 2022;38(2):423–438. doi:10.1016/j.ijforecast.2020.08.004
7. Bjørnskov C. Did lockdown work? An economist's cross-country comparison. *CESifo Econ Stud*. 2021;67(3):318–331. doi:10.1093/cesifo/ifab003
8. Dowell SF. Seasonal variation in host susceptibility and cycles of certain infectious diseases. *Emerg Infect Dis*. 2001;7(3):369–374. doi:10.3201/eid0703.017301
9. Shaman J, Kohn M. Absolute humidity modulates influenza survival, transmission, and seasonality. *Proc Natl Acad Sci U S A*. 2009;106(9):3243–3248. doi:10.1073/pnas.0806852106
10. Tamerius JD, Shaman J, Alonso WJ, Bloom-Feshbach K, Uejio CK, Comrie A. Environmental predictors of seasonal influenza epidemics across temperate and tropical climates. *PLoS Pathog*. 2011;7(3):e1002154. doi.org/10.1371/journal.ppat.1003194
11. Box GEP. Science and statistics. *J Am Stat Assoc*. 1976;71(356):791–799. doi:10.1080/01621459.1976.10480949

12. Leon DA, Shkolnikov VM, Smeeth L, Magnus P, Pechholdová M, Jarvis CI. COVID-19: a need for real-time monitoring of weekly excess deaths. *Lancet*. 2020;395(10234):e81. doi:10.1016/S0140-6736(20)30933-8
13. Sterman JD. *Business dynamics: systems thinking and modeling for a complex world*. Boston: Irwin/McGraw-Hill; 2000.
14. Liu Y, Gayle AA, Wilder-Smith A, Rocklöv J. The reproductive number of COVID-19 is higher compared to SARS coronavirus. *J Travel Med*. 2020;27(2):taaa021. doi:10.1093/jtm/taaa021
15. European Centre for Disease Prevention and Control (ECDC). COVID-19 surveillance data [Internet]. Stockholm: ECDC; 2020–2025 [cited 2025 Jan]. Available from: https://www.ecdc.europa.eu/en/covid-19/data
16. The COVID Tracking Project. The COVID Tracking Project at *The Atlantic* [Internet]. 2020–2021 [cited 2025 Jan]. Available from: https://covidtracking.com

Supplement

S1 Fig.
Core simulation settings in Stella Architect.
Screenshot of the *Stella Architect* model settings used for SEVA simulations, including numerical integration method (Euler).
In the graphical window on the right, the sigmoidal curvature (1.00) and the duration (40 days) are fixed for all simulations, whereas p_max is varied (in this example set to 0.05).

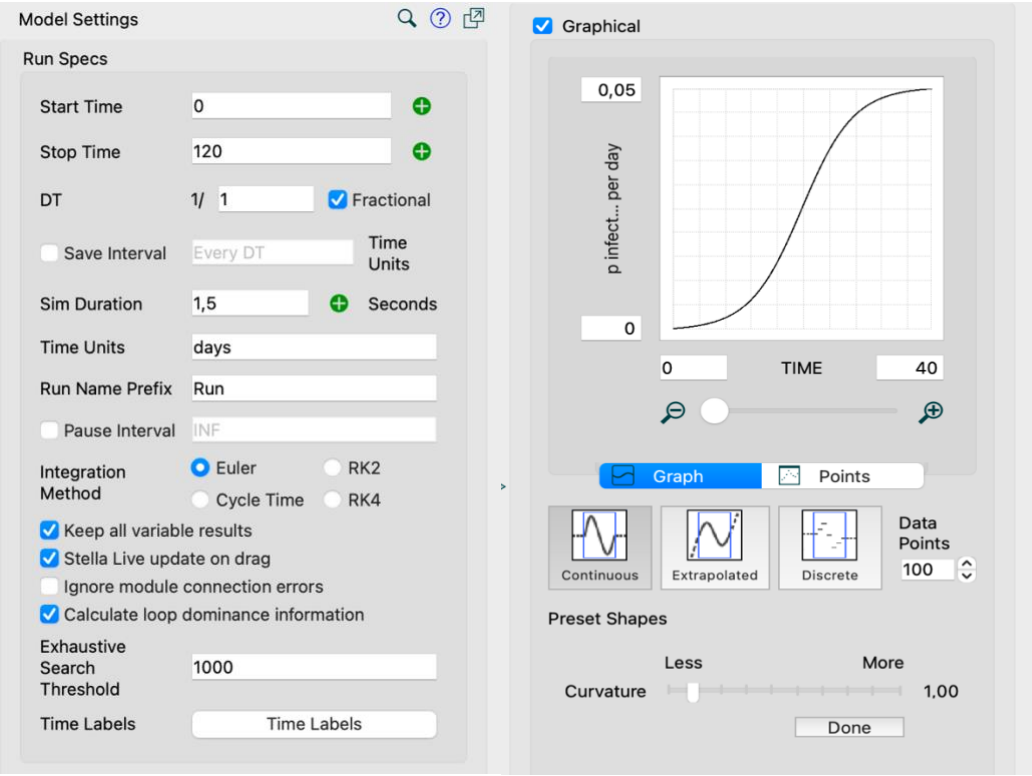

S2 Fig SEVA model fits to daily COVID-19 mortality (7-day average, per 100,000) for 13 additional European countries during the first epidemic wave. Curves are aligned to 8 March 2020; differences in wave shape are captured by variation in p_max.

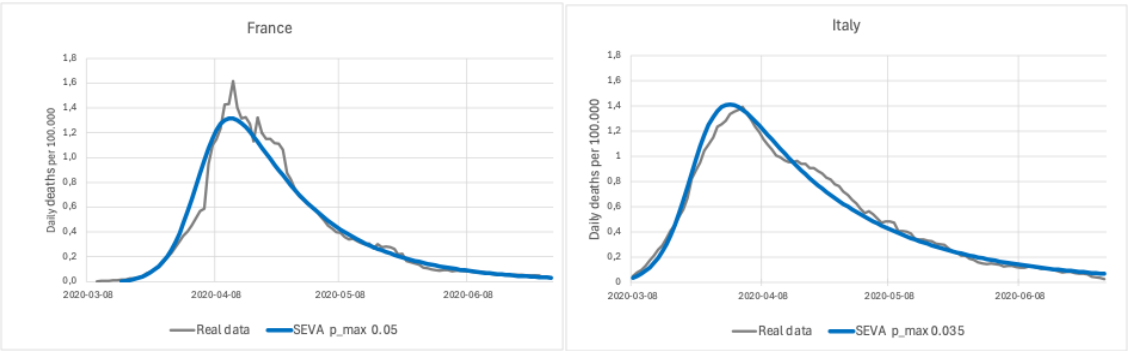

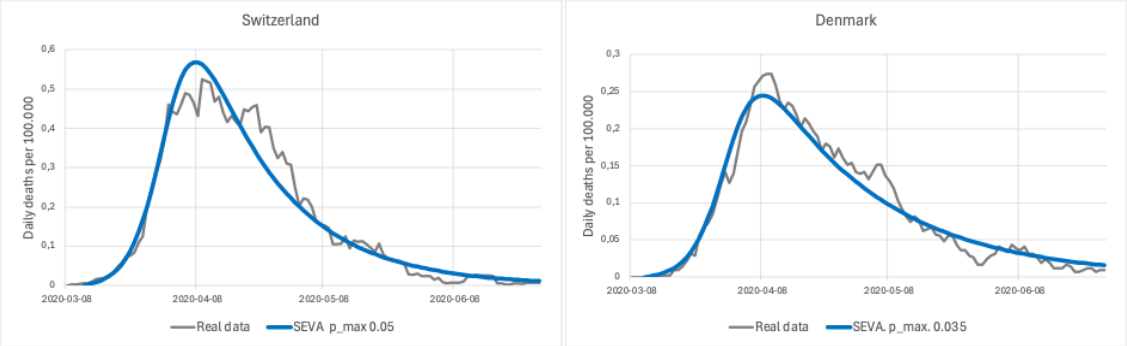

531

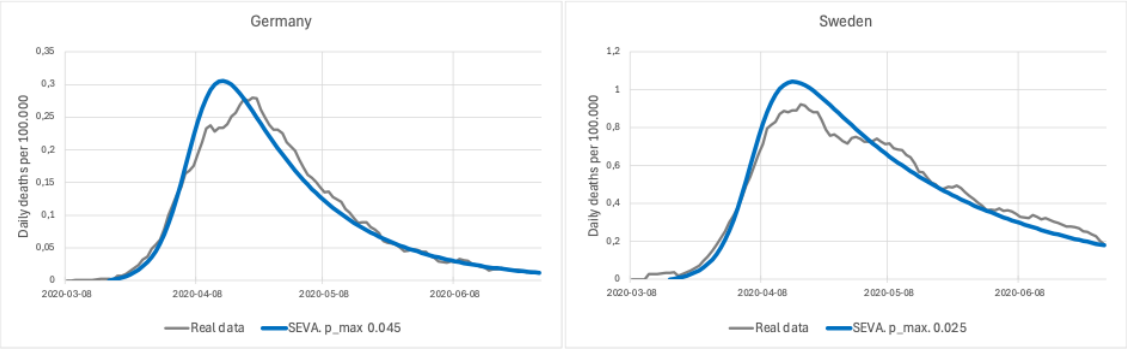

532

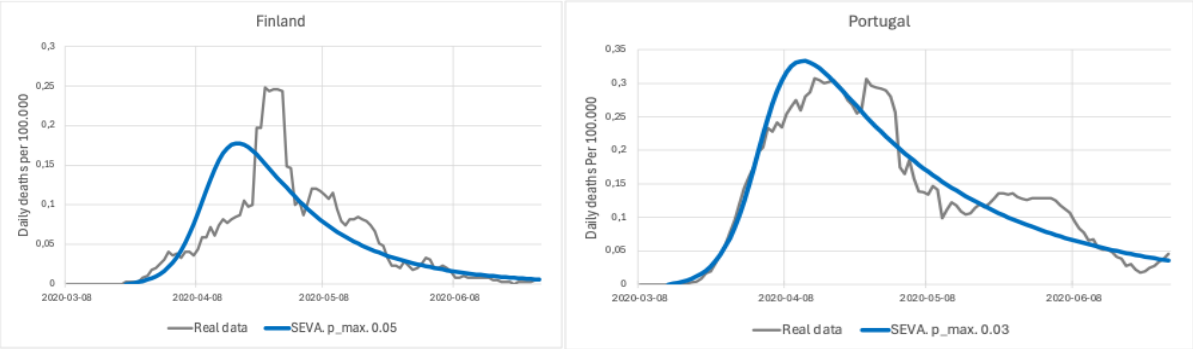

533

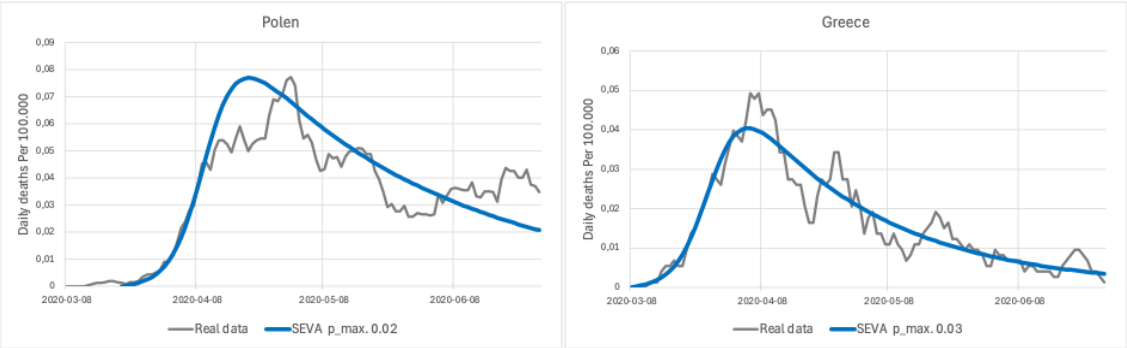

534

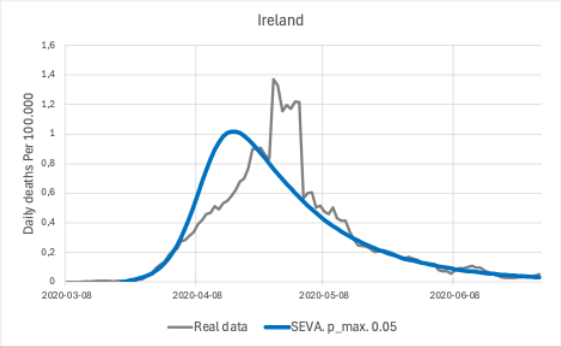
Ireland
Daily deaths Per 100.000
1,6
1,4
1,2
1
0,8
0,6
0,4
0,2
0
2020-03-08
2020-04-08
2020-05-08
2020-06-08
Real data
SEVA. p_max. 0.05

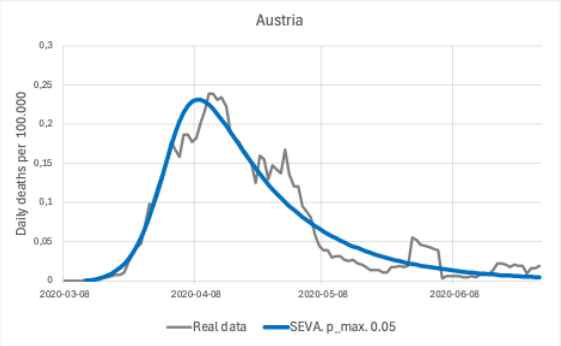
Austria
Daily deaths per 100.000
0,3
0,25
0,2
0,15
0,1
0,05
0
2020-03-08
2020-04-08
2020-05-08
2020-06-08
Real data
SEVA. p_max. 0.05

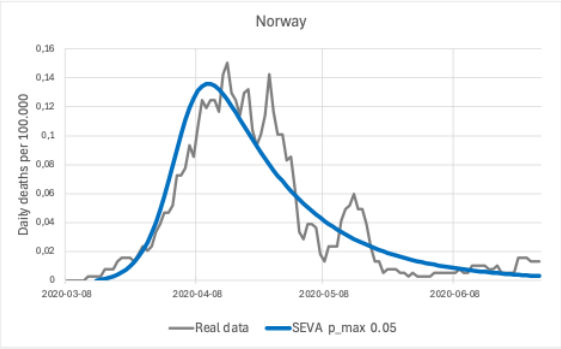
Norway
Daily deaths per 100.000
0,16
0,14
0,12
0,1
0,08
0,06
0,04
0,02
0
2020-03-08
2020-04-08
2020-05-08
2020-06-08
Real data
SEVA p_max 0.05